

Supporting information

A one-dimensional organic-inorganic hybrid ferroelectric exhibiting dielectric-optical duplex switch

Qian-Jun Gu, Yu-Qiao Tong, Shi-Qing Yin, Ping Wang, Peng-Peng Gong, Ya-Juan Li, Yue Fang, Yang Zhao and Bo Huang*

Yunnan Key Laboratory of Modern Separation Analysis and Substance Transformation, College of Chemistry and Chemical Engineering, Yunnan Normal University, Kunming 650500, China.

Materials and instrumentations. All chemicals were obtained from commercial sources and used without further purification. Powder X-Ray diffraction (PXRD) pattern (Cu-K α , $\lambda = 1.54056 \text{ \AA}$) was collected on a Smartlab9 θ - 2θ diffractometer. IR spectra was carried out on SHIMADZU IRPrestige-21. Thermogravimetric (TG) analysis was performed on a TA Q50 system at a heating rate of 5 K/min under a N₂ atmosphere. Differential scanning calorimetry (DSC) were measured by cooling-heating the powder sample at a rate of 5 K/min on a NETZSCH DSC200 F3 instrument. Single-crystal X-ray data at 193 K and 260 K were performed on RAXIS IP diffractometer with Mo-K α radiation ($\lambda = 0.71073 \text{ \AA}$). The complex permittivity ($\epsilon = \epsilon' - i\epsilon''$, ϵ' is the real part and ϵ'' is the imaginary part) were measured using a Tonghui TH2838A LCR meter (applied electric field of 1.0 V) connected to a cryogenic environment controller for a powder-pressed sample at a rate of about 3 K/min at various frequencies (1, 2, 4, 6, 8, 10, 20, 40, 60, 80, 100, 200, 400, 600, 800, 10000 kHz). Second harmonic generation (SHG) was measured using a WITec alpha 300RS microscope with a 1064 nm laser. The pyroelectric current was measured with Keithley 6517B electrometer. The ferroelectric hysteresis loop was recorded on aixACCT/ TF-2000E.

Synthesis. A methanol solution (30 mL) containing stoichiometric quantities of BiCl₃ (10 mmol), pyrrolidine (20 mmol), and HCl (20 mmol) were stirred for about 20 minutes. The clear solution was allowed to evaporate slowly at room temperature. After a few days, colorless columnar crystals of (C₄H₈NH₃)₂BiCl₅ (**1**) were obtained in about 81% yield (based on Bi).

Calculation of ΔS and N . The total heat Q (3.561/3.465 J g⁻¹ for the cooling/heating process) was obtained by integrating the heat flow with respect to temperature using the analysis software of NETZSCH DSC200 F3 instrument. According to the Boltzmann equation, $\Delta S = R \ln(N)$, $M_r = 530.49 \text{ g mol}^{-1}$, $R = 8.314 \text{ J mol}^{-1} \text{ K}^{-1}$, $T_c(\text{Heating}) = 228.0 \text{ K}$, $T_c(\text{Cooling}) = 225.0 \text{ K}$, the calculated entropy

change ΔS and number of possible orientations N from the DSC is about 8.3/8.2 J mol⁻¹ K⁻¹ and 2.7/2.7 for the cooling/heating process.

In the heating cycle process:

$$\begin{aligned}\Delta S_H &= R \ln N_H \\ &= \int_{T_2}^{T_1} \frac{Q}{T} dT \\ &= \frac{3.561 \text{ J.g}^{-1} \times 530.49 \text{ g.mol}^{-1}}{228.0 \text{ K}} \\ &\approx 8.3 \text{ J.mol}^{-1} \text{K}^{-1}\end{aligned}$$

$$\begin{aligned}N_H &= \exp\left(\frac{\Delta S_H}{R}\right) \\ &= \exp\frac{8.2854 \text{ J.mol}^{-1} \text{K}^{-1}}{8.314 \text{ J.mol}^{-1} \text{K}^{-1}} \\ &\approx 2.7\end{aligned}$$

In the cooling cycle process:

$$\begin{aligned}\Delta S_C &= R \ln N_C \\ &= \int_{T_2}^{T_1} \frac{Q}{T} dT \\ &= \frac{3.465 \text{ J.g}^{-1} \times 530.49 \text{ g.mol}^{-1}}{225.0 \text{ K}} \\ &\approx 8.2 \text{ J.mol}^{-1} \text{K}^{-1}\end{aligned}$$

$$\begin{aligned}N_C &= \exp\left(\frac{\Delta S_C}{R}\right) \\ &= \exp\frac{8.1695 \text{ J.mol}^{-1} \text{K}^{-1}}{8.314 \text{ J.mol}^{-1} \text{K}^{-1}} \\ &\approx 2.7\end{aligned}$$

Theoretical calculation. Density functional theory (DFT) calculations were performed using the GaussView software to construct the molecular structure of the compound, and performing calculations use Gaussian software, which required optimization to achieve the most stable conformation with minimal energy. Subsequently, the 6-31G (d) basis set and B3LYP functional were selected to refine the geometric structures of various polymer molecules. Once the molecular

conformation is determined, the electric dipole moment of the anions, cations, and the entire system will be calculating. The sum of the electric dipole moments per unit volume is the polarization, measured in $\mu\text{C}/\text{cm}^2$. The projector augmented wave method¹ was employed with the Perdew-Burke-Ernzerhof (PBE) generalized gradient approximation functional.² The energy cutoff was set to 350 eV, and a $2 \times 4 \times 4$ Monkhorst-Pack grid of k points was used. The Berry phase approach was employed to calculate the ferroelectric polarization P .³

Table S1. Summary of crystal data and structural refinements of **1** at 193 and 260 K.

Empirical formula	(C ₄ H ₈ NH ₂) ₂ [BiCl ₅]	
Formula weight	530.49	
Phase type	LTP	HTP
<i>T</i> / K	193(2)	260(2)
Space group	<i>Pna</i> 2 ₁	<i>Pcmn</i>
<i>a</i> / Å	36.5385(6)	18.2766(2)
<i>b</i> / Å	15.7813(3)	8.0882(4)
<i>c</i> / Å	11.6585(2)	11.7414(7)
<i>V</i> / Å ³	6722.6(2)	1735.7(2)
<i>Z</i>	4	2
<i>D</i> _{calcd} / g cm ⁻³	2.097	2.030
<i>μ</i> / mm ⁻¹	11.266	10.908
GOF	1.033	1.029
<i>R</i> ₁ , <i>wR</i> ₂ [<i>I</i> > 2σ(<i>I</i>)] ^a	0.0341, 0.0542	0.0527, 0.1339
<i>R</i> ₁ , <i>wR</i> ₂ (all data)	0.0626, 0.0585	0.0789, 0.1498
Flack parameter	0.460(4)	–
CCDC No	2393673	2393674

$$^a R_1 = F_o - F_c / F_o, wR_2 = \{w[(F_o)^2 - (F_c)^2]^2 / w[(F_o)^2]\}^{1/2}$$

Table S2. The selected bond lengths (Å) of **1** at 193 and 260 K.

193 K	Bi1–Cl1	2.576(2)	Bi1–Cl2	2.738(2)
	Bi1–Cl3	2.542(2)	Bi1–Cl4	2.660(2)
	Bi1–Cl5	2.888(2)	Bi1–Cl16 ¹	2.925(2)
	Bi2–Cl5	2.864(2)	Bi2–Cl6	2.544(2)
	Bi2–Cl7	2.802(2)	Bi2–Cl8	2.611(2)
	Bi2–Cl9	2.583(2)	Bi2–Cl10	2.930(2)
	Bi3–Cl10	2.807(2)	Bi3–Cl11	2.577(2)
	Bi3–Cl12	2.727(2)	Bi3–Cl13	2.614(2)
	Bi3–Cl14	2.681(2)	Bi3–Cl15	2.859(2)
	Bi4–Cl15	2.899(2)	Bi4–Cl16	2.899(2)
	Bi4–Cl17	2.632(2)	Bi4–Cl18	2.571(2)
	Bi4–Cl19	2.758(2)	Bi4–Cl20	2.561(2))
	260 K	Bi1–Cl1	2.86(8)	Bi1–Cl1 ²
Bi1–Cl1 ³		2.95(8)	Bi1–Cl1 ⁴	2.86(8)
Bi1–Cl2		2.662(6)	Bi1–Cl2 ⁴	2.662(6)
Bi1–Cl3		2.547(3)	Bi1–Cl3 ⁴	2.547(3)
Bi1–Cl4		2.729(5)		

Symmetry code: ¹+x,-1+y,+z; ²+x, -1/2-y, +z; ³+x,-1/2-y,+z; ⁴-1-x,-1/2+y,1-z**Table S3.** The selected bond angles (°) of **1** at 193 and 260 K.

193 K	∠Cl1–Bi1–Cl2	88.33(8)	∠Cl1–Bi1–Cl3	92.35(7)
	∠Cl1–Bi1–Cl4	91.48(7)	∠Cl1–Bi1–Cl5	176.42(7)
	∠Cl1–Bi1–Cl16 ¹	91.89(8)	∠Cl2–Bi1–Cl3	88.88(8)
	∠Cl2–Bi1–Cl4	177.93(8)	∠Cl2–Bi1–Cl5	92.02(7)
	∠Cl2–Bi1–Cl16 ¹	90.62(9)	∠Cl3–Bi1–Cl4	93.20(7)
	∠Cl3–Bi1–Cl5	91.23(6)	∠Cl3–Bi1–Cl16 ¹	175.72(9)
	∠Cl4–Bi1–Cl5	88.04(6)	∠Cl4–Bi1–Cl16 ¹	87.32(8)
	∠Cl5–Bi2–Cl6	86.60(7)	∠Cl5–Bi2–Cl16 ¹	84.54(9)
	∠Cl5–Bi2–Cl7	87.90(6)	∠Cl5–Bi2–Cl8	86.88(7)

$\angle \text{Cl5-Bi2-Cl9}$	179.11(7)	$\angle \text{Cl5-Bi2-Cl10}$	86.79(7)
$\angle \text{Cl6-Bi2-Cl7}$	87.97(8)	$\angle \text{Cl6-Bi2-Cl8}$	90.69(9)
$\angle \text{Cl6-Bi2-Cl9}$	94.29(8)	$\angle \text{Cl6-Bi2-Cl10}$	172.29(7)
$\angle \text{Cl7-Bi2-Cl8}$	174.68(7)	$\angle \text{Cl7-Bi2-Cl9}$	92.16(7)
$\angle \text{Cl7-Bi2-Cl10}$	87.83(6)	$\angle \text{Cl8-Bi2-Cl9}$	93.08(8)
$\angle \text{Cl8-Bi2-Cl10}$	92.90(7)	$\angle \text{Cl9-Bi2-Cl10}$	92.32(7)
$\angle \text{Cl10-Bi3-Cl11}$	87.80(7)	$\angle \text{Cl10-Bi3-Cl12}$	87.09(7)
$\angle \text{Cl10-Bi3-Cl13}$	176.68(7)	$\angle \text{Cl10-Bi3-Cl14}$	90.98(7)
$\angle \text{Cl10-Bi3-Cl15}$	88.95(7)	$\angle \text{Cl11-Bi3-Cl12}$	91.54(9)
$\angle \text{Cl11-Bi3-Cl13}$	94.07(8)	$\angle \text{Cl11-Bi3-Cl14}$	90.20(9)
$\angle \text{Cl11-Bi3-Cl15}$	176.64(8)	$\angle \text{Cl12-Bi3-Cl13}$	90.12(7)
$\angle \text{Cl12-Bi3-Cl14}$	90.09(7)	$\angle \text{Cl12-Bi3-Cl15}$	89.14(7)
$\angle \text{Cl13-Bi3-Cl14}$	91.76(8)	$\angle \text{Cl13-Bi3-Cl15}$	89.22(7)
$\angle \text{Cl14-Bi3-Cl15}$	89.01(7)	$\angle \text{Cl15-Bi4-Cl16}$	86.15(8)
$\angle \text{Cl15-Bi4-Cl17}$	88.41(7)	$\angle \text{Cl15-Bi4-Cl18}$	85.73(7)
$\angle \text{Cl15-Bi4-Cl19}$	87.18(7)	$\angle \text{Cl15-Bi4-Cl20}$	179.73(7)
$\angle \text{Cl16-Bi4-Cl17}$	88.41(8)	$\angle \text{Cl16-Bi4-Cl18}$	171.01(9)
$\angle \text{Cl16-Bi4-Cl19}$	95.18(9)	$\angle \text{Cl16-Bi4-Cl20}$	93.83(8)
$\angle \text{Cl17-Bi4-Cl18}$	87.51(8)	$\angle \text{Cl17-Bi4-Cl19}$	174.12(7)
$\angle \text{Cl17-Bi4-Cl20}$	91.85(8)	$\angle \text{Cl18-Bi4-Cl19}$	88.28(8)
$\angle \text{Cl18-Bi4-Cl20}$	94.31(8)	$\angle \text{Cl19-Bi4-Cl20}$	92.56(7)
$\angle \text{Cl1-Bi1-Cl1}^2$	95.00(2)	$\angle \text{Cl1-Bi1-Cl2}$	92.00(2)

260 K

$\angle \text{Cl1-Bi1-Cl2}^2$	83.00(2)	$\angle \text{Cl1-Bi1-Cl3}$	86.20(1)
$\angle \text{Cl1-Bi1-Cl3}^2$	178.20(1)	$\angle \text{Cl1-Bi1-Cl4}$	90.80(2)
$\angle \text{Cl2-Bi1-Cl2}^2$	11.60(7)	$\angle \text{Cl2-Bi1-Cl3}$	95.80(3)
$\angle \text{Cl2-Bi1-Cl3}^2$	87.40(3)	$\angle \text{Cl2-Bi1-Cl4}$	173.60(3)
$\angle \text{Cl2}^1\text{-Bi1-Cl4}$	173.60(3)	$\angle \text{Cl3-Bi1-Cl3}^2$	92.30(2)
$\angle \text{Cl3-Bi1-Cl4}$	90.28(2)	$\angle \text{Cl3}^2\text{-Bi1-Cl4}$	95.70(2)

Symmetry code: $^1+x,-1+y,+z$; $^2+x,-1/2-y,+z$

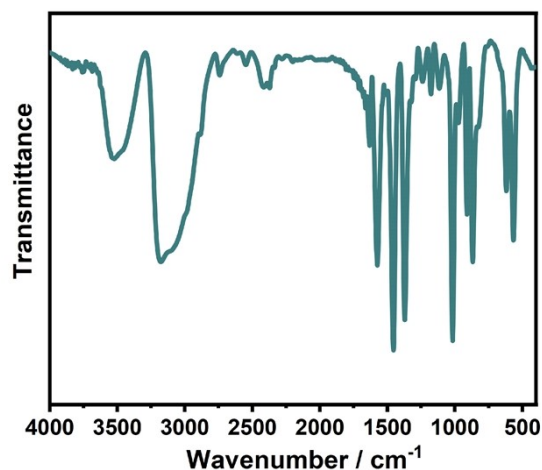


Fig. S1 IR spectra of **1**. The peaks observed at 3533 cm^{-1} , 3180 cm^{-1} , and 1371 cm^{-1} could be attributed to the stretching vibrations of N–H, C–H, and C–N, respectively. The peaks observed at 1573 cm^{-1} , 1454 cm^{-1} , 1016 cm^{-1} , and 867 cm^{-1} could be assigned to the bending vibration of N–H, $-\text{CH}_2-$, in-plane C–H, and out-of-plane C–H, respectively.

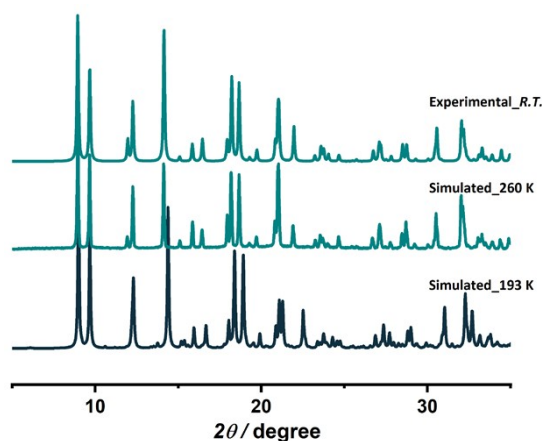


Fig. S2 The simulated (193 and 260 K) and experimental powder XRD patterns of **1**.

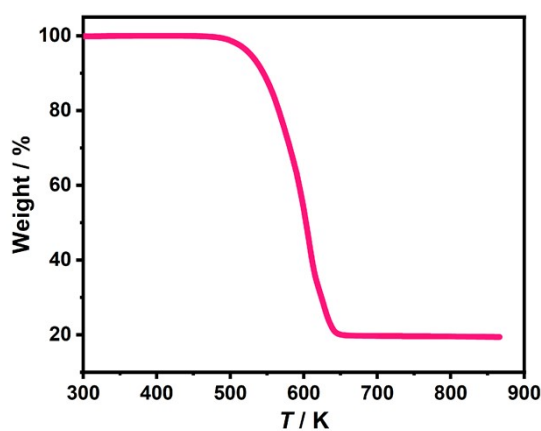


Fig. S3 Thermogravimetric (TG) curve measured at a rate of 5 K min^{-1} under N_2 atmosphere of **1**. It reveals that compound **1** was stable up to about 480 K.

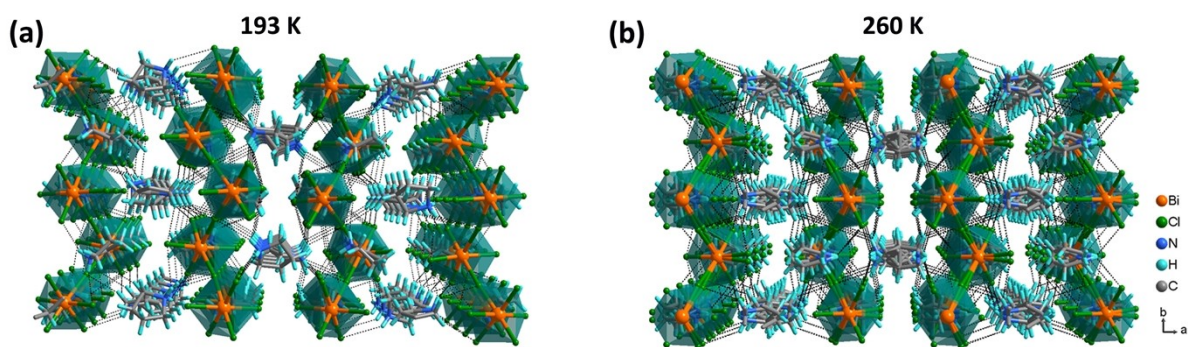


Fig. S4 The packing diagram of **1** at 193 and 260 K. The black dotted lines represent hydrogen bonds.

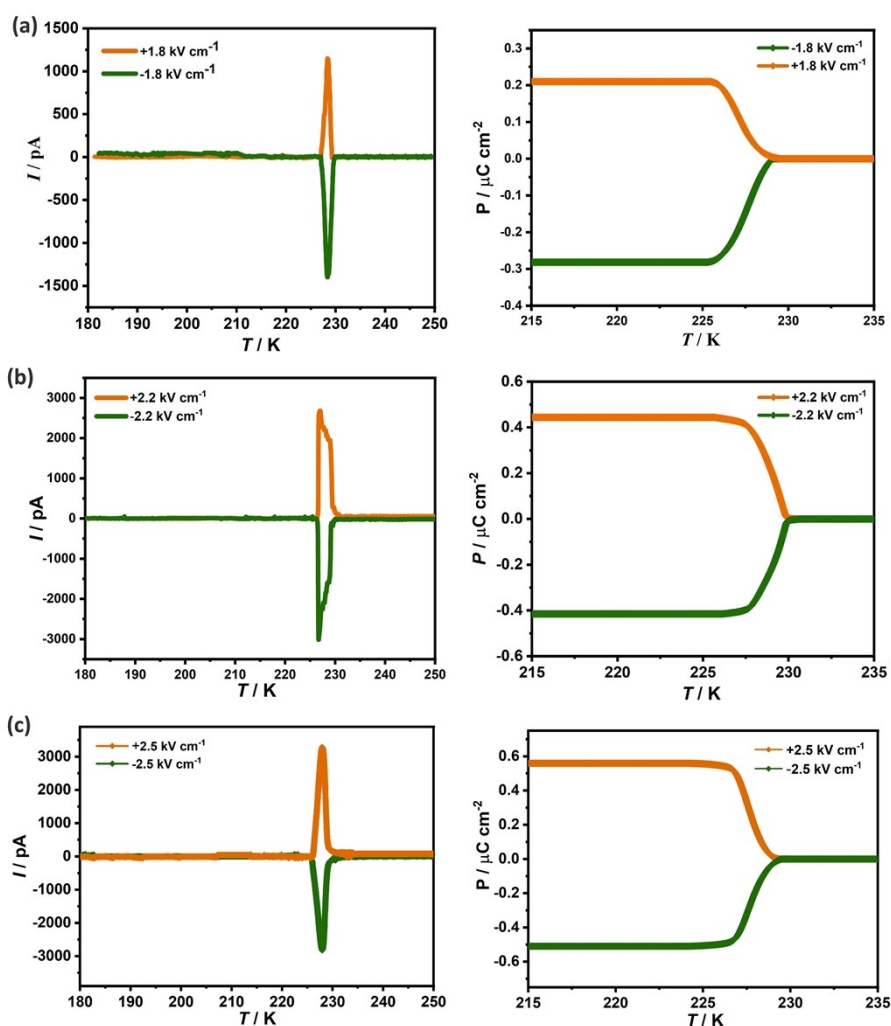


Fig. S5 The temperature dependent pyroelectric current and spontaneous polarization of **1** at different poled voltages measured approximately along the *c*-axis. The pyroelectric current (*I*) was obtained from heating mode under zero electric field in the vicinity of the ferroelectric phase transition. Before measuring the pyroelectric current, the sample was cooled down from about 250

K to 180 K with an applied electric field of about $\pm 1.8 \text{ kV cm}^{-1}$ (a), 2.2 kV cm^{-1} (b) and 2.5 kV cm^{-1} (c), respectively. By integrating the pyroelectric current with respect to time, spontaneous polarizations (P) of about $0.21 \text{ } \mu\text{C cm}^{-2}$ (a), $0.44 \text{ } \mu\text{C cm}^{-2}$ (b), and $0.56 \text{ } \mu\text{C cm}^{-2}$ (c) were obtained.

References

1. Blöchl, P. E. Projector augmented-wave method. *Phys. Rev. B: Condens. Matter Mater. Phys.* 1994, **50**, 17953.
2. Perdew, J. P.; Burke, K.; Ernzerhof, M. Generalized Gradient Approximation Made Simple. *Phys. Rev. Lett.* 1996, **77**, 3865.
3. King-Smith, R. D.; Vanderbilt, D. Theory of polarization of crystalline solids. *Phys. Rev. B: Condens. Matter Mater. Phys.* 1993, **47**, 1651.